The Journal of Chemical Physics

Path integral description of semiflexible active Brownian polymers

Cite as: J. Chem. Phys. **156**, 064105 (2022); https://doi.org/10.1063/5.0081020
Submitted: 06 December 2021 • Accepted: 25 January 2022 • Accepted Manuscript Online: 25 January 2022 • Published Online: 09 February 2022

Thomas Eisenstecken and Roland G. Winkler

The Journal of Chemical Physics ARTICLE scitation.org/journal/jcp

Path integral description of semiflexible active Brownian polymers

Cite as: J. Chem. Phys. 156, 064105 (2022); doi: 10.1063/5.0081020
Submitted: 6 December 2021 • Accepted: 25 January 2022 •
Published Online: 9 February 2022

Thomas Eisenstecken and Roland G. Winkler

AFFILIATIONS

Theoretical Physics of Living Matter, Institute of Biological Information Processing and Institute for Advanced Simulation, Forschungszentrum Jülich, D-52425 Jülich, Germany

Author to whom correspondence should be addressed: r.winkler@fz-juelich.de

ABSTRACT

Semiflexible polymers comprised of active Brownian particles (ABPOs) exhibit intriguing activity-driven conformational and dynamical features. Analytically, the generic properties of ABPOs can be obtained in a mean-field description applying the Gaussian semiflexible polymer model. In this article, we derive a path integral representation of the stationary-state distribution function of such ABPOs, based on the stationary-state distribution function of the normal mode amplitudes following from the Langevin equation of motion. The path integral includes characteristic semiflexible polymer contributions from entropy and bending energy, with activity dependent coefficients, and, in addition, activity-induced torsional and higher order correlations along the polymer contour. Focusing on a semiflexible polymer approximation, we determine various properties such as the tangent-vector correlation function, effective persistence length, and the mean-square end-to-end distance. The latter reflects the characteristic features of ABPOs, and good quantitative agreement is obtained with the full solution for larger activities, specifically for flexible polymers. Moreover, the approximation indicates the relevance of torsional and higher order contour correlations for the ABPO conformations. In general, the ABPO path integral illustrates how colored noise (active fluctuations) affects semiflexible polymer conformations in comparison to white noise thermal fluctuations.

I. INTRODUCTION

Living matter is characterized by a multitude of complex dynamical processes maintaining its out-of-equilibrium nature.[1,2] Molecular machines such as (motor) proteins and ribosomes undergo conformational changes fueled by Adenosine Triphosphate (ATP), which drive and stir the cell interior.[3,4] This triggers a hierarchy of dynamical processes, movements, and transport, resulting in a nonequilibrium state of the cell—from the molecular to the whole-cell level—[2] with intriguing collective phenomena emerging by migration and locomotion also on scales much larger than individual cells.[5–10] The nature of living and active matter systems implies nonthermal fluctuations, broken detailed balance, and a violation of the dissipation–fluctuation relation, which renders their theoretical description particularly challenging.[2,10]

Filaments and polymers are an integral part of biological systems, with active processes affecting their conformational and dynamical properties.[10] Forces generated by kinesin motors walking along microtubule filaments affect the dynamics of the cytoskeletal network and produce nonequilibrium conformational fluctuations also of actin filaments,[11,12] which ultimately contribute to the organization of the cell interior.[10,13–17] In DNA transcription, ATPases such as DNA or RNA polymerase (RNAP, DNAP) move along the DNA, which generates nonthermal fluctuations for both, RNAP/DNAP and the transcribed DNA.[18–20] Various ATP-dependent processes affect the dynamics of chromosomal loci[21,22] and chromatin.[23] Moreover, spatial segregation of active (euchromatin) and passive (heterochromatin) chromatin has been found.[24–26] These aspects suggest that active processes are essential for the cell function.[27]

Various theoretical[28–36] and simulation[28,37–45] studies have been performed to elucidate the conformational and dynamical properties of linear and ring polymers comprised of active Brownian particles, in the presence and absence of hydrodynamic interactions. Most remarkable are the strong polymer conformational changes, with swelling of flexible polymers with increasing activity, shrinkage of semiflexible polymers at moderate activity, and swelling at larger activities in an identical manner as flexible polymers.[10,31,32]

Dynamically, activity leads to a ballistic polymer center-of-mass mean-square displacement,[10,32] and in particular, in the presence of hydrodynamic interactions, additionally yields an internal power-law monomer displacement different from those of a passive system.[40,42]

All approaches are based on dynamical equations, typically Langevin equations for the particle positions and their orientations, which naturally also yield stationary-state properties. In contrast, for passive systems, the polymer conformational properties can be derived from statistical physics only, and the partition function can be presented in the form of a path integral. Here, the question arises, whether a similar description of the stationary-state properties of ABPOs is possible.

In this article, we show that the conformational properties of ABPOs can indeed be described by a path integral and integration over configurational space. In particular, we show that the active polymer can approximately be considered as a semiflexible polymer for sufficiently large activities. We characterize the polymer conformational properties by calculating the tangent-vector correlation function, the effective persistence length, and the mean-square end-to-end distance. These properties reflect the characteristic features of ABPOs in very good quantitative agreement with the full solution of the Langevin equation, in particular, for flexible polymers and larger activities for all polymer stiffnesses. Deviations for moderate, stiffness-dependent activities are a consequence of the neglect of torsional interactions and higher order correlations along the polymer in the semiflexible polymer path integral representation. Here, our calculations reveal the effect of such higher order correlations on the ABPO conformational properties, an aspect not considered so far.

In general, by the path integral representation of ABPOs, established concepts for passive polymers can be applied to analyze and characterize their conformational properties. Particularly, the comparison with passive semiflexible polymers emphasizes the effect of activity on the polymer conformations. Strikingly, it reveals the impact of colored noise (active fluctuations) on the polymer conformations in comparison to thermal fluctuations of passive polymers.

II. ACTIVE BROWNIAN POLYMER MODEL

A. Equation of motion

The active Brownian polymer (ABPO) is modeled in a mean-field manner as a Gaussian semiflexible polymer—a three dimensional, continuous, differentiable space curve $\boldsymbol{r}(s,t)$ of length L with the contour coordinate s $(-L/2 < s < L/2)$ evolving in time, t,[46–52]—argument by a local active velocity $\boldsymbol{v}(s,t)$.[10,31,32,36] The overdamped Langevin equation of the ABPO in a thermal bath is given by[10,31,32,36]

$$\frac{\partial}{\partial t}\boldsymbol{r}(s,t) = \boldsymbol{v}(s,t) + \frac{1}{\gamma}\left(2\nu k_B T\frac{\partial^2}{\partial s^2}\boldsymbol{r}(s,t) - \epsilon k_B T\frac{\partial^4}{\partial s^4}\boldsymbol{r}(s,t) + \boldsymbol{\Gamma}(s,t)\right) \tag{1}$$

with the free-end boundary conditions[31,32,50]

$$\left[2\nu\frac{\partial}{\partial s}\boldsymbol{r}(s,t) - \epsilon\frac{\partial^3}{\partial s^3}\boldsymbol{r}(s,t)\right]_{\pm L/2} = 0, \tag{2}$$

$$\left[2\nu_0\frac{\partial}{\partial s}\boldsymbol{r}(s,t) \pm \epsilon\frac{\partial^2}{\partial s^2}\boldsymbol{r}(s,t)\right]_{\pm L/2} = 0. \tag{3}$$

The terms with the second and fourth derivatives in Eq. (1) account for the conformational entropy and bending energy, respectively. For the stretching coefficient ν_0 and the bending coefficient ϵ, we set $\nu_0 = 3/4$ and $\epsilon = 3l_p/2 = 3/(4p)$, where $l_p = 1/(2p)$ is the persistence length of the passive polymer.[52] The stretching coefficient ν is determined in a mean-field manner by the global constraint of a finite ABPO contour length,[31,52–54]

$$\int_{-L/2}^{L/2}\left\langle\left(\frac{\partial\boldsymbol{r}(s,t)}{\partial s}\right)^2\right\rangle ds = L. \tag{4}$$

The thermal force $\boldsymbol{\Gamma}(s,t)$ is assumed to be stationary, Markovian, and Gaussian with zero mean and the second moments,

$$\left\langle\Gamma_\alpha(s,t)\Gamma_\beta(s',t')\right\rangle = 2\gamma k_B T\delta_{\alpha\beta}\delta(s-s')\delta(t-t'), \tag{5}$$

where T is the temperature, k_B is the Boltzmann constant, γ is the translational friction coefficient per length, and $\alpha,\beta \in \{x,y,z\}$.

The dynamics of the active velocity $\boldsymbol{v}(s,t)$ is described by an Ornstein–Uhlenbeck process (AOBP),[6,31,55–57] with a vanishing first moment, $\langle\boldsymbol{v}(s,t)\rangle = 0$, and the correlation function (colored noise),

$$\left\langle\boldsymbol{v}(s,t)\cdot\boldsymbol{v}(s',t')\right\rangle = v_0^2 l e^{-\gamma_R(t-t')}\delta(s-s'). \tag{6}$$

Here, v_0 denotes the magnitude of the active velocity, l can be related to the number of active sites $N = L/l$ along the polymer, and $\gamma_R = 2D_R$ in three dimensions, with D_R being the rotational diffusion coefficient.[10,31] Hence, Eq. (1) is a stochastic differential equation of a semiflexible polymer in the presence of white (thermal) and colored (active) noise.

B. Solution of the equations of motion: Eigenfunction expansion

The linear equation (1) is easily solved by an eigenfunction expansion,[10,31,32,50]

$$\boldsymbol{r}(s,t) = \sum_{n=0}^{\infty}\boldsymbol{\chi}_n(t)\varphi_n(s), \tag{7}$$

in terms of the eigenfunctions $\varphi_n(s)$ of the equation

$$\epsilon k_B T\frac{d^4}{ds^4}\varphi_n(s) - 2\nu k_B T\frac{d^2}{ds^2}\varphi_n(s) = \xi_n\varphi_n(s). \tag{8}$$

Explicitly, the eigenfunctions are given by[50]

$$\varphi_0 = \sqrt{\frac{1}{L}}, \tag{9}$$

$$\varphi_n(s) = \sqrt{\frac{c_n}{L}}\left(\zeta_n'\frac{\sinh\zeta_n' s}{\cosh\zeta_n' L/2} + \zeta_n\frac{\sin\zeta_n s}{\cos\zeta_n L/2}\right),\ n \text{ odd}, \tag{10}$$

$$\varphi_n(s) = \sqrt{\frac{c_n}{L}}\left(\zeta_n'\frac{\cosh\zeta_n' s}{\sinh\zeta_n' L/2} - \zeta_n\frac{\cos\zeta_n s}{\sin\zeta_n L/2}\right),\ n \text{ even}, \tag{11}$$

with the wave numbers ζ_n, ζ_n', and the eigenvalues ξ_n,

$$\zeta_n'^2 - \zeta_n^2 = \frac{2\nu}{\epsilon}, \quad \xi_0 = 0, \quad \xi_n = k_B T(\epsilon\zeta_n^4 + 2\nu\zeta_n^2). \tag{12}$$

The wave numbers ζ_n, ζ_n' are specified by the boundary conditions [Eqs. (2) and (3)], and the constants c_n are normalization coefficients.[32,50] The eigenfunction φ_0 accounts for a polymer's translational motion. Note that ξ_n depend on the stretching coefficient ν, which is a function of activity due to the constraint (4).[31,32,56]

Equation (1) yields the equations of motion for the mode amplitudes $\boldsymbol{\chi}_n$,

$$\frac{d}{dt}\boldsymbol{\chi}_n(t) = -\frac{1}{\tau_n}\boldsymbol{\chi}_n(t) + \boldsymbol{v}_n(t) + \frac{1}{\gamma}\boldsymbol{\Gamma}_n(t), \tag{13}$$

with the relaxation times

$$\tau_n = \frac{\gamma}{\xi_n} = \frac{\gamma}{k_B T(\epsilon\zeta_n^4 + 2\nu\zeta_n^2)}, \tag{14}$$

and the normal mode amplitudes $\boldsymbol{v}_n$, $\boldsymbol{\Gamma}_n$ of the active velocities and stochastic forces, respectively. The mode amplitude $\boldsymbol{v}_n(t)$ satisfies the equation of motion

$$\frac{d}{dt}\boldsymbol{v}_n(t) = -\gamma_R \boldsymbol{v}_n(t) + \boldsymbol{\Xi}_n(t) \tag{15}$$

with the correlation functions

$$\langle \boldsymbol{\Xi}_n(t) \cdot \boldsymbol{\Xi}_m(0)\rangle = 2\gamma_R v_0^2 l \delta_{nm}\delta(t - t') \tag{16}$$

of the normal mode amplitudes of the Gaussian and Markovian stochastic process $\boldsymbol{\Xi}(s,t)$ of zero mean.[31]

The stationary-state solution of Eq. (13) is

$$\boldsymbol{\chi}_n(t) = e^{-t/\tau_n}\int_{-\infty}^{t} e^{t'/\tau_n}\left(\boldsymbol{v}_n(t') + \frac{1}{\gamma}\boldsymbol{\Gamma}_n(t')\right)dt', \tag{17}$$

which yields the stationary-state mean-square average,[31,32]

$$\langle \boldsymbol{\chi}_n^2(t)\rangle = \frac{3k_B T\tau_n}{\gamma} + \frac{v_0^2 l \tau_n^2}{1 + \gamma_R\tau_n}. \tag{18}$$

C. Stationary-state distribution function of mode amplitudes

Equations (13) and (15) are coupled Ornstein–Uhlenbeck processes with an exact analytical solution in terms of a Gaussian.[57,58] Integration over the velocity modes, $\boldsymbol{v}_n$, yields the stationary-state Gaussian distribution function for the normal mode amplitudes $\boldsymbol{\chi}_n$,

$$\psi(\{\boldsymbol{\chi}_n\}) = \prod_{n=1}^{\infty}\left(\frac{3}{2\pi\langle\boldsymbol{\chi}_n^2\rangle}\right)^{3/2}\exp\left(-\frac{3}{2}\sum_{m=1}^{\infty}\frac{\boldsymbol{\chi}_m^2}{\langle\boldsymbol{\chi}_m^2\rangle}\right), \tag{19}$$

with $\langle\boldsymbol{\chi}_n^2\rangle$ of Eq. (18).

III. PATH INTEGRAL REPRESENTATION OF ABPO

A path integral representation of the active Brownian polymer is obtained by exploiting the eigenvalue equation (8). We focus on the limit, where the active term with v_0^2 dominates the correlation function of Eq. (18), i.e., we neglect the thermal contribution and use $\langle\boldsymbol{\chi}_n^2\rangle = v_0^2 l\tau_n^2/(1 + \gamma_R\tau_n)$. Hence, the term in the exponent of Eq. (19) becomes

$$\sum_{n=1}^{\infty}\frac{\boldsymbol{\chi}_n^2}{\langle\boldsymbol{\chi}_n^2\rangle} = \frac{1}{v_0^2 l\gamma^2}\sum_{n=1}^{\infty}(\xi_n^2 + \gamma_R\gamma\xi_n)\boldsymbol{\chi}_n^2. \tag{20}$$

The two terms on the right-hand side of Eq. (20) can be transformed into

$$\sum_{n=1}^{\infty}\xi_n^2\boldsymbol{\chi}_n^2 = \int_{-L/2}^{L/2}(\mathcal{O}\boldsymbol{r}(s))^T\mathcal{O}\boldsymbol{r}(s)\,ds, \tag{21}$$

$$\sum_{n=1}^{\infty}\xi_n\boldsymbol{\chi}_n^2 = \int_{-L/2}^{L/2}\boldsymbol{r}(s)^T\mathcal{O}\boldsymbol{r}(s)\,ds \tag{22}$$

by using the orthonormality of the eigenfunctions and the abbreviation,

$$\mathcal{O} = \epsilon k_B T\frac{d^4}{ds^4} - 2\nu k_B T\frac{d^2}{ds^2}. \tag{23}$$

Insertion of the operator, partial integration, and exploitation of the boundary conditions lead to the path integral representation of the distribution function in terms of the position $\boldsymbol{r}(s)$ (cf. the Appendix),

$$\begin{aligned}\psi(\{\boldsymbol{r}\}) = \frac{1}{Z}\exp\Bigg(&-\frac{3k_B T}{v_0^2 l\gamma^2}\Bigg[\nu\gamma\gamma_R\int_{-L/2}^{L/2}\left(\frac{\partial\boldsymbol{r}}{\partial s}\right)^2 ds \\ &+ \frac{4k_B T\nu^2 + \gamma\gamma_R\epsilon}{2}\int_{-L/2}^{L/2}\left(\frac{\partial^2\boldsymbol{r}}{\partial s^2}\right)^2 ds \\ &+ 2k_B T\nu\epsilon\int_{-L/2}^{L/2}\left(\frac{\partial^3\boldsymbol{r}}{\partial s^3}\right)^2 ds + \frac{k_B T\epsilon^2}{2}\int_{-L/2}^{L/2}\left(\frac{\partial^4\boldsymbol{r}}{\partial s^4}\right)^2 ds \\ &+ v_0\left(\gamma_R\gamma + \frac{8k_B T\nu^2}{\epsilon}\right)\left[\left(\frac{\partial\boldsymbol{r}}{\partial s}\right)_{L/2}^2 + \left(\frac{\partial\boldsymbol{r}}{\partial s}\right)_{-L/2}^2\right]\Bigg]\Bigg).\end{aligned} \tag{24}$$

$Z = \int\exp(\cdots)\mathcal{D}^3 r$ is the partition function, with the dots representing the exponent in Eq. (24) and $\mathcal{D}^3 r$ being the integration over paths.[49,59,60] Aside from the characteristic terms of semiflexible polymers (first and second derivatives), Eq. (24) includes higher order derivatives accounting for torsion (third derivative) and longer range correlations (fourth derivative) along the polymer contour. The partition function can be evaluated because of the Gaussian nature of the integrand, but the derivation of a closed-form expression based on the path integral is involved. In any case, we can calculate the partition function via the eigenfunction representation. Here, we focus on a semiflexible polymer representation of our active polymer neglecting torsional and higher order correlations, i.e., a distribution function of the form

$$\begin{aligned}\psi(\{\boldsymbol{r}\}) = \frac{1}{Z}\exp\Bigg(&-\tilde{\nu}\int_0^L\left(\frac{\partial\boldsymbol{r}}{\partial s}\right)^2 ds - \frac{\tilde{\epsilon}}{2}\int_0^L\left(\frac{\partial^2\boldsymbol{r}}{\partial s^2}\right)^2 ds \\ &- \tilde{v}_0\left[\left(\frac{\partial\boldsymbol{r}}{\partial s}\right)_L^2 + \left(\frac{\partial\boldsymbol{r}}{\partial s}\right)_0^2\right]\Bigg)\end{aligned} \tag{25}$$

with the abbreviations

$$\tilde{\nu} = \frac{3k_BT\nu\gamma_R}{v_0^2 l\gamma}, \tag{26}$$

$$\tilde{\epsilon} = \frac{3k_BT}{v_0^2 l\gamma^2}(4k_BT\nu^2 + \gamma\gamma_R\epsilon), \tag{27}$$

$$\tilde{\nu}_0 = \frac{3k_BT\nu_0}{v_0^2 l\gamma^2}\left(\gamma\gamma_R + \frac{8k_BT\nu^2}{\epsilon}\right). \tag{28}$$

The parameter ϵ depends on the flexibility and ν additionally in a nonlinearly manner on the activity of the ABPO. Note that we changed the integration interval in Eq. (25) from $-L/2 \le s \le L/2$ to $0 \le s \le L$.

IV. GREEN'S FUNCTION

Averages are conveniently calculated via Green's function $G(\boldsymbol{r},\boldsymbol{u},s|\boldsymbol{r}',\boldsymbol{u}',s')$, which is the conditional probability distribution function of the position $\boldsymbol{r} = \boldsymbol{r}(s)$ and derivative $\boldsymbol{u} = \boldsymbol{u}(s) = \partial\boldsymbol{r}/\partial s$ given the values $\boldsymbol{r}' = \boldsymbol{r}(s')$, $\boldsymbol{u}' = \boldsymbol{u}(s')$. In terms of the path integral, Green's function reads

$$G(\boldsymbol{r},\boldsymbol{u},s|\boldsymbol{r}',\boldsymbol{u}',s') = \frac{1}{Z_G}\int_{\boldsymbol{r}',\boldsymbol{u}'}^{\boldsymbol{r},\boldsymbol{u}} \exp\left(-\tilde{\nu}\int_{s'}^{s}\left(\frac{\partial\boldsymbol{r}}{\partial s''}\right)^2 ds'' - \frac{\tilde{\epsilon}}{2}\int_{s'}^{s}\left(\frac{\partial^2\boldsymbol{r}}{\partial s''^2}\right)^2 ds''\right)\mathcal{D}^3 r, \tag{29}$$

with fixed points $\boldsymbol{r},\boldsymbol{r}'$ and "tangents" $\boldsymbol{u},\boldsymbol{u}'$. The normalization factor Z_G ensures that $G(\boldsymbol{r},\boldsymbol{u},s'|\boldsymbol{r}',\boldsymbol{u}',s') = \delta(\boldsymbol{r}-\boldsymbol{r}')\delta(\boldsymbol{u}-\boldsymbol{u}')$.[49] The path integral (29) is a Markov process, and Green's function obeys the Chapman–Kolmogorov equation.[58] Green's function can be obtained via a discrete representation of the path integral and integration or as the solution of the partial differential equation for G.[49,59,60] Explicitly, it is given by $(0 < s' < s < L)$,

$$G(\boldsymbol{r},\boldsymbol{u},s|\boldsymbol{r}',\boldsymbol{u}',s') = \frac{1}{Z_G^r(s-s')}G(\boldsymbol{u},s|\boldsymbol{u}',s')\exp\left(-\tilde{\nu}\frac{\left[\boldsymbol{r}-\boldsymbol{r}'-(\boldsymbol{u}+\boldsymbol{u}')\sqrt{\tilde{\epsilon}/2\tilde{\nu}}\tanh(\sqrt{\tilde{\nu}/2\tilde{\epsilon}}(s-s'))\right]^2}{s-s'-\sqrt{2\tilde{\epsilon}/\tilde{\nu}}\tanh(\sqrt{\tilde{\nu}/2\tilde{\epsilon}}(s-s'))}\right), \tag{30}$$

with Green's function for the tangent vectors

$$G(\boldsymbol{u},s|\boldsymbol{u}',s') = \frac{1}{Z_G^u(s-s')}\exp\left(-\frac{\sqrt{\tilde{\nu}\tilde{\epsilon}/2}}{\sinh(\sqrt{2\tilde{\nu}/\tilde{\epsilon}}(s-s'))} \times\left[(\boldsymbol{u}^2+\boldsymbol{u}'^2)\cosh(\sqrt{2\tilde{\nu}/\tilde{\epsilon}}(s-s')) - 2\boldsymbol{u}\cdot\boldsymbol{u}'\right]\right) \tag{31}$$

and the normalization factors $(Z_G = Z_G^r Z_G^u)$

$$Z_G^u(s) = \left(\frac{\pi\sinh(\sqrt{2\tilde{\nu}/\tilde{\epsilon}}s)}{\sqrt{\tilde{\nu}\tilde{\epsilon}/2}}\right)^{3/2}, \qquad Z_G^r(s) = \left(\frac{\pi\left[s-\sqrt{2\tilde{\epsilon}/\tilde{\nu}}\tanh(\sqrt{\tilde{\nu}/2\tilde{\epsilon}}s)\right]}{\tilde{\nu}}\right)^{3/2}. \tag{32}$$

V. JOINT PROBABILITY DISTRIBUTION

The joint probability distribution function $\psi(\boldsymbol{u},s;\boldsymbol{u}',s')$ for the tangent vectors $\boldsymbol{u}$ at s and $\boldsymbol{u}'$ at s' is calculated by exploiting the Markov property of Green's function (30), which yields

$$\psi(\boldsymbol{u},s;\boldsymbol{u}',s') = \frac{1}{Z_{uu'}}\int e^{-\tilde{\nu}_0\boldsymbol{u}_L^2}G(\boldsymbol{u}_L,L|\boldsymbol{u},s)G(\boldsymbol{u},s|\boldsymbol{u}',s') \times G(\boldsymbol{u}',s'|\boldsymbol{u}_0,0)e^{-\tilde{\nu}_0\boldsymbol{u}_0^2}d^3u_L d^3u_0, \tag{33}$$

where $Z_{uu'}$ is the normalization factor, $\boldsymbol{u}_L = \boldsymbol{u}(L)$, and $\boldsymbol{u}_0 = \boldsymbol{u}(0)$. The exponential functions with $\tilde{\nu}_0$ account for the distribution of the "tangent" vectors at the polymer ends [cf. Eqs. (24) and (25)]. Integration yields

$$\psi(\boldsymbol{u},s;\boldsymbol{u}',s') = \frac{1}{Z_{uu'}}\exp\left(-\frac{\tilde{\epsilon}\kappa}{2\sinh(\kappa(s-s'))}\left[\frac{\phi(L-s')}{\phi(L-s)}\boldsymbol{u}^2 + \frac{\phi(s)}{\phi(s')}\boldsymbol{u}'^2 - 2\boldsymbol{u}\cdot\boldsymbol{u}'\right]\right) \tag{34}$$

with the abbreviations $\kappa = \sqrt{2\tilde{\nu}/\tilde{\epsilon}}$,

$$\phi(s) = \tilde{\nu}_0\sinh(\kappa s) + \frac{1}{2}\tilde{\epsilon}\kappa\cosh(\kappa s) \tag{35}$$

and the normalization factor

$$Z_{uu'} = \left(\frac{2\sinh(\kappa(s-s'))\phi(L-s)\phi(s')}{\tilde{\nu}\tilde{\epsilon}[(\tilde{\nu}_0^2+\tilde{\nu}\tilde{\epsilon}/2)\sinh(\kappa L)+\tilde{\nu}_0\tilde{\epsilon}\kappa\cosh(\kappa L)]}\right)^{3/2}. \tag{36}$$

The probability distribution function $\psi(\boldsymbol{u})$ of the tangent vector is obtained by integration of Eq. (34) over $\boldsymbol{u}'$ and yields a Gaussian for $\boldsymbol{u}(s)$ with the mean-square average

$$\langle\boldsymbol{u}^2(s)\rangle = \frac{3}{4\tilde{\epsilon}\kappa}\frac{[2\tilde{\nu}_0\sinh(\kappa s)+\tilde{\epsilon}\kappa\cosh(\kappa s)][2\tilde{\nu}_0\sinh(\kappa(L-s))+\tilde{\epsilon}\kappa\cosh(\kappa(L-s))]}{[\tilde{\nu}_0^2+\tilde{\nu}\tilde{\epsilon}/2]\sinh(\kappa L)+\tilde{\epsilon}\tilde{\nu}_0\kappa\cosh(\kappa L)]}. \tag{37}$$

VI. CONFORMATIONAL PROPERTIES

A. Stretching coefficient

The activity dependence of the stretching coefficient ν is obtained from the constraint (4). Integration of Eq. (37) over the polymer contour s yields the equation

$$\frac{3}{4\tilde{\epsilon}\kappa}\frac{\left[2\tilde{v}_0\tilde{\epsilon}\kappa L+\tilde{v}\tilde{\epsilon}/\kappa-2\tilde{v}_0^2/\kappa\right]\sinh(\kappa L)+\left[2\tilde{v}_0^2L+\tilde{v}\tilde{\epsilon}L\right]\cosh(\kappa L)}{\left[\tilde{v}_0^2+\tilde{v}\tilde{\epsilon}/2\right]\sinh(\kappa L)+\tilde{\epsilon}\tilde{v}_0\kappa\,\cosh(\kappa L)}=L, \tag{38}$$

which has to be solved numerically, in general.

Figure 1 displays the normalized stretching coefficient $\mu = 2\nu/(3p)$ as a function of activity for various pL. We use the Péclet number Pe and the ratio Δ to characterize activity, where

$$Pe=\frac{v_0}{lD_R},\quad \Delta=\frac{D_T}{l^2D_R} \tag{39}$$

with the translational diffusion coefficient $D_T = k_BT/(\gamma l)$. In the following, we will use $\Delta = 1/3$, corresponding to the ratio of the thermal diffusion coefficients of a spherical colloid of diameter l in a fluid. In general, D_T and D_R can be chosen independently. Stiffness is characterized by the ration $L/l_p = 2pL$ of the polymer length and the persistence length as measured in the passive state ($Pe \to 0$). Only data for $Pe > 3$ are provided because the approximation in Eq. (20) applies for $Pe \gg 1$ only.

The stretching coefficient derived from the path integral representation agrees well with the exact solution obtained via the solution of the Langevin equation (1).[31] As the exact solution, Eq. (38) yields the dependence on the Péclet number,

$$\mu=\frac{Pe^{4/3}N}{6pL\Delta} \tag{40}$$

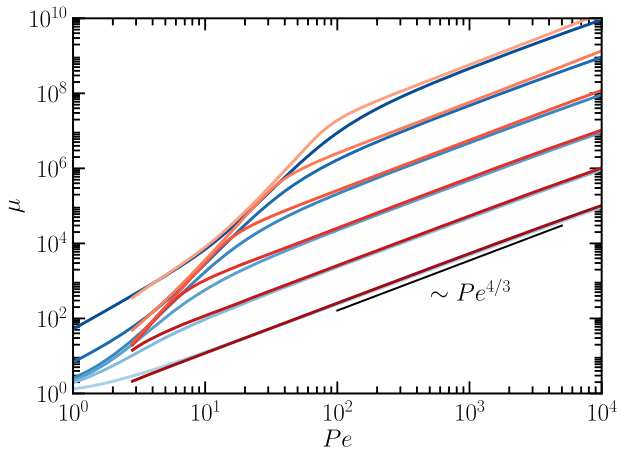

FIG. 1. Normalized stretching coefficient (Lagrangian multiplier) $\mu = 2\nu/3p$ as a function of the Péclet number Pe for polymers of various stiffnesses with $pL = 10^3, 10^2, 10, 1, 10^{-1}$, and 10^{-2} (bottom to top). For the other parameters, we set $N = L/l = 10^3$ and $\Delta = 1/3$. The red curves are obtained from Eq. (38) of the path integral representation, and the blue curves represent the results obtained as a sum of the eigenfunctions as described in Ref. 31. The black line indicates the power-law $\mu \sim Pe^{4/3}$.

for Pe, $\mu < \infty$ and $pL \to \infty$. In the limit $Pe \to \infty$ and $0 < pL < \infty$, the analytical approximation of Eq. (38) yields

$$\mu=Pe\sqrt{\frac{N^3}{54(pL)^2\Delta^2}}\sqrt{\frac{2pL+3+3/(4pL)}{2pL+1}}, \tag{41}$$

with an additional term (second square root on the right-hand side) compared to the exact solution.[31] Clearly, this term is irrelevant for flexible polymers, where $pL \gg 1$, but yields a deviation from the exact result for $pL < 1$.

The apparent difference with the exact solution for smaller $Pe \lesssim 3$ is a consequence of the applied large Pe approximation (Fig. 1). However, for intermediate Pe, in the crossover regime to $\mu \sim Pe^{4/3}$ and in the limit $Pe \to \infty$, the neglected torsional term and the term with the fourth derivative in the path integral yield a visible contribution.

Figure 1 presents a broad range of Péclet numbers to illustrate the asymptomatic behavior for large Pe. For an estimation of the Péclet number in cellular systems, we consider the action of ATPases on chromatin motion.[17] For such a system, the definition of Pe changes to $Pe = Fl/(k_BT)$, where F is the force exerted by a molecular motor, l is its step length, and k_BT is the thermal energy. Using $F \approx 10$ pN and $l \approx 10$ nm yields $Pe \approx 20$ at room temperature. A similar value has been used in Ref. 17. For a (hypothetical) synthetic polymer comprised of freely rotating Janus particles, Eq. (39) gives the larger value $Pe \approx 10^2$ with the swim velocity $v \approx 5$ μm/s, the diameter $l \approx 5$ μm, and the rotational diffusion coefficient $D_R \approx 10^{-2}$ s^{-1} in water at room temperature. Possible restrictions in the rational diffusion coefficient by bonds would increase the Péclet number, and not too large velocities are required to achieve even larger Pe. As shown in Fig. 1 (and the following figures), in the range of $Pe = 10^1$–10^2, the polymers exhibit already strong activity effects.

B. Mean-square tangent vector

An inextensible polymer contour implies the constraint $|\boldsymbol{u}(s)| = 1$ or, under relaxed (mean filed) conditions, the constraint $\langle \boldsymbol{u}^2(s)\rangle = 1$.[49,59,61] The latter relation is satisfied for the passive Gaussian semiflexible polymer adopted here for all s ($0 \le s \le L$).[49] As a consequence, the global constraint (4) captures the inextensibility of the polymer equivalently to the local constraint.[49] However, external forces or active forces may render the two approaches—local constraints vs global constraint—inequivalent,[52] and, under the global constraint, the polymer contour may deform (stretch/compress) inhomogeneously.

Figure 2 presents the mean-square tangent vector as a function of the contour coordinate for various Péclet numbers and pL values. For $Pe \lesssim 10$, $\langle \boldsymbol{u}^2\rangle$ deviates appreciably from unity for stiffer polymers ($pL = 0.1$). Above $pL = 1$, the deviations are within a few percent only, aside from strong chain end effects. In general, for $Pe > 50$, the deviation from unit is smaller than 5% for all pL, aside from end effects, with largest deviations for $pL \lesssim 1$ and $pL > 10$. Independent of Pe, we find pronounced chain end effects with a severe drop or increase in the mean-square tangent vector as a consequence of the applied global constraint. In general, the parameter ν depends on the position s in the presence of forces.[52] Nevertheless, the local constraint $\langle \boldsymbol{u}^2\rangle = 1$ is surprisingly well satisfied considering the strong

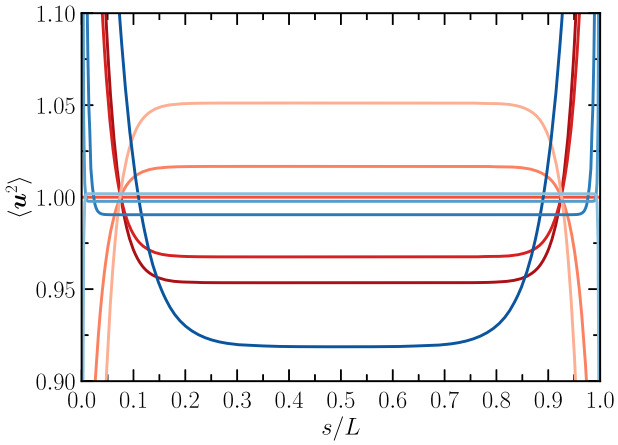

FIG. 2. Mean-square tangent vector $\langle \boldsymbol{u}^2(s) \rangle$ as a function of the contour coordinate s/L for $Pe = 10$ (blue) and $Pe = 10^3$ (red) and the polymer length to stiffness ratios $pL = 0.1, 1, 5$(red), $10, 10^3$ (dark to bright). Curves for $pL > 10^3$ deviate only slightly from those for $pL = 10^3$.

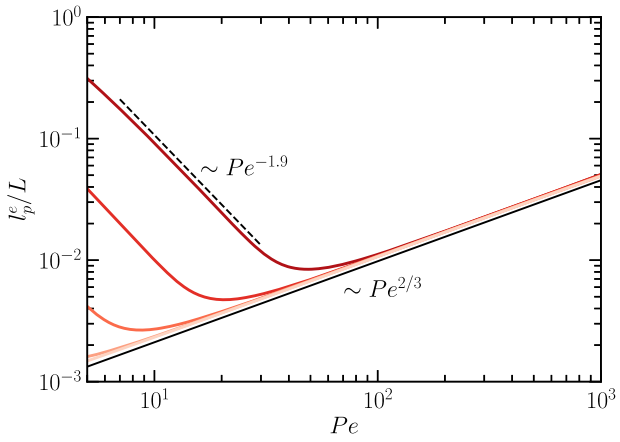

FIG. 3. Effective persistence length as a function of the Péclet number for the polymer stiffnesses $pL = 0.1, 1, 10, 10^2$, and 10^3 (dark to bright). The solid line indicates the power-law dependence $Pe^{2/3}$, and the dashed line indicates the dependence $Pe^{-1.9}$.

polymer conformational changes with increasing activity. The pronounced variations at the polymer ends are of minor importance for properties on the scale of the whole polymer for most of the Pe and pL values. The change in $\langle \boldsymbol{u}^2 \rangle$ from values <1 to values >1 reflect the compression of stiffer polymers and the stretching of flexible polymers by the activity.

C. Tangent vector correlation function

The tangent vector correlation function $\langle \boldsymbol{u} \cdot \boldsymbol{u}' \rangle$ is as follows:

$$\langle \boldsymbol{u} \cdot \boldsymbol{u}' \rangle = \frac{3\phi(L-s)\phi(s')}{\tilde{\epsilon}\kappa[(\tilde{\nu}_0^2 + \tilde{\nu}\tilde{\epsilon}/2)\sinh(\kappa L) + \tilde{\nu}_0\tilde{\epsilon}\kappa\cosh(\kappa L)]} \tag{42}$$

via the joint probability distribution in Eq. (34). This expression turns into the mean-square tangent vector (37) for $s' = s$. Factoring out the exponential with the positive exponent in the hyperbolic functions, the correlation function can be written as

$$\frac{\langle \boldsymbol{u} \cdot \boldsymbol{u}' \rangle}{\langle \boldsymbol{u}^2 \rangle} = \frac{2\tilde{\nu}_0(1 - e^{-2\kappa s'}) + \tilde{\epsilon}\kappa(1 + e^{-2\kappa s'})}{2\tilde{\nu}_0(1 - e^{-2\kappa s}) + \tilde{\epsilon}\kappa(1 + e^{-2\kappa s})} e^{-\kappa|s-s'|}. \tag{43}$$

For $2\kappa s, 2\kappa s' \gg 1$ or $2\kappa s, 2\kappa s' \ll 1$, the normalized correlation function decays exponentially, and we can introduce the effective persistence length $l_p^e = 1/\kappa$ with

$$\kappa L = \sqrt{\frac{2\,N^3}{pL\mu\Delta}} \Big/ \sqrt{1 + \frac{N^3}{6(pL)^3\mu^2\Delta}}, \tag{44}$$

a function of the Péclet number and polymer stiffness.

The dependence of the effective persistence length on the Péclet number is displayed in Fig. 3. Evidently, l_p^e/L is significantly smaller than the unit for $pL > 1$ ($Pe > 10$ for $pL = 0.1$). Using $s/L, s'/L < 1$, the relation $2\,s/l_p^e, 2\,s'/l_p^e \gg 1$ is satisfied for not too small s, s' and the correlation decays exponentially, as confirmed by a numerical evaluation of the tangent vector correlation function. The polymer end regimes ($s/L \approx 0, 1$) should be considered with care in the calculation of a persistence length, as the mean-square tangent vector (Fig. 2) deviates considerably from unity.

For flexible polymers ($pL \approx N$) and/or large Péclet numbers ($\mu \gg 1$), the square-root term in the denominator of Eq. (44) is unity and $l_p^e \sim \sqrt{\mu}$. Since $\mu \sim Pe^{4/3}$ for $\kappa L \gg 1$ (Sec. VI A), the effective persistence length increases as $l_p^e \sim Pe^{2/3}$ with the Péclet number, i.e., with increasing Pe, the active polymer becomes stiffer (Fig. 3). In contrast, l_p^e of semiflexible polymers decreases over a certain range of (small) Pe values with increasing Péclet number. Here, the square-root term in the denominator of Eq. (44) dominates and $l_p^e \sim 1/\sqrt{\mu}$, which for increasing μ yields a decreasing l_p^e.

D. Mean-square end-to-end distance

The polymer mean-square end-to-end distance, $\langle \boldsymbol{R}_e^2 \rangle = \langle (\boldsymbol{r}(L) - \boldsymbol{r}(0))^2 \rangle$, can be calculated from the tangent vector correlation function (42) via

$$\langle \boldsymbol{R}_e^2 \rangle = \int_0^L \int_0^L \langle \boldsymbol{u}(s) \cdot \boldsymbol{u}(s') \rangle ds ds', \tag{45}$$

which yields (cf. Ref. 52)

$$\langle \boldsymbol{R}_e^2 \rangle = \frac{3}{2\tilde{\nu}} \left(L - \frac{2\tilde{\nu}_0}{\tilde{\nu}} \left[1 + \frac{\tilde{\nu}_0\kappa}{\tilde{\nu}} \coth(\kappa L/2) \right]^{-1} \right). \tag{46}$$

The dependence of $\langle \boldsymbol{R}_e^2 \rangle$ on the Péclet number is displayed in Fig. 4 for various values of pL. Qualitatively, good agreement is obtained between the path integral mean-square end-to-end distance and the full solution via the eigenfunction expansion. In particular, the approach reproduces the shrinkage of $\langle \boldsymbol{R}_e^2 \rangle$ of stiff polymers at small Pe, as well as the swelling of flexible and semiflexible polymers with increasing Pe. Quantitatively, we observe differences in the crossover regime from shrinkage to swelling. Moreover, the asymptotic value for $Pe \to \infty$ of the path integral approach deviates from the limit $\langle \boldsymbol{R}_e^2 \rangle = L^2/2$ of the eigenfunction approach. All

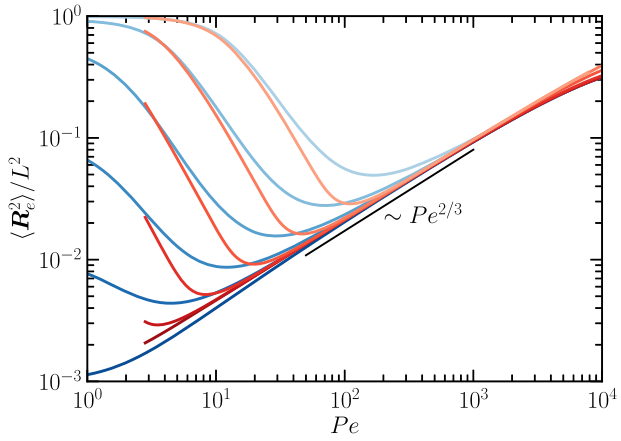

FIG. 4. Polymer mean-square end-to-end distance as a function of the Péclet number. Comparison of the path integral result (red), Eq. (46), with the $\langle \boldsymbol{R}_e^2 \rangle$ values obtained from the solution of the Langevin equation (blue)[31] for $pL = 10^{-2}$, $0.1, 1, 10, 10^2$, and 10^3 (bright to dark). The solid line indicates the power-law dependence $Pe^{2/3}$.

the deviations for $Pe \gtrsim 5$ are attributed to the neglected higher order derivatives in Eq. (25). As for the full solution, the mean-square end-to-end distance (46) yields

$$\langle \boldsymbol{R}_e^2 \rangle = \frac{Pe^2}{6pL\mu\Delta} \tag{47}$$

for $\mu \gg 1$ and $1 \ll Pe < \infty$. With the Pe dependence $\mu \sim Pe^{4/3}$ (Fig. 1), the mean-square end-to-end increases as $\langle \boldsymbol{R}_e^2 \rangle / L^2 \sim Pe^{2/3}$ over a certain range of Pe values.

To illustrate the thermal contribution, $3k_BT\tau_n/\gamma$, to the mean-square end-to-end distance, in Fig. 5, we compare the full mean-square end-to-end distance obtained from the Langevin equation with the approximation (47). Evidently, the latter relation captures

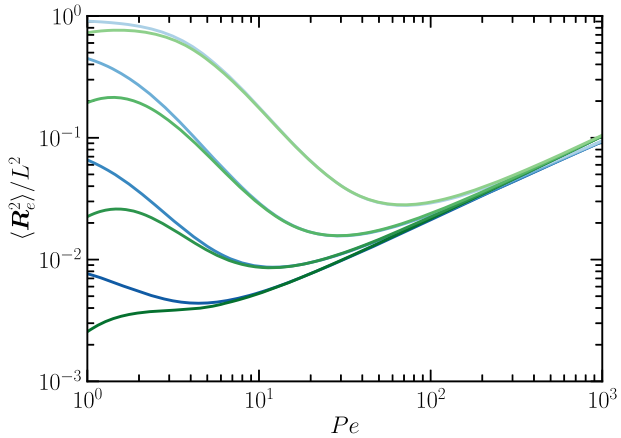

FIG. 5. Mean-square end-to-end distance obtained from the solution of the Langevin equation (blue) and via the approximation in Eq. (47) (green) for $pL = 0.1, 1, 10$, and 10^2 (bright to dark).

the Péclet number dependence of $\langle \boldsymbol{R}_e^2 \rangle$ over a wide range of Pe values very well. Note that the $\langle \boldsymbol{R}_e^2 \rangle$ curves are calculated with the stretching coefficient, μ, of the eigenfunction solution (Fig. 1, blue). Only for $Pe \lesssim 5$, the approximation underestimates the full solution, where the discrepancy increases with increasing polymer flexibility. Thus, the mean-square end-to-end distance is solely determined by the active term in Eq. (18) for $Pe \gtrsim 5$.

Since the thermal contribution to $\langle \boldsymbol{R}_e^2 \rangle$ shows the dependence $\tau_n \sim 1/\mu(Pe)$ for $Pe \gg 1$ [Eq. (14)] and μ increases monotonically with Pe, the thermal contribution decreases monotonically with increasing Pe.[40] The approximation (47) applies for not too large Pe values only. The asymptotic limit $Pe \to \infty$, $\mu \sim Pe^2$, and $\langle \boldsymbol{R}_e^2 \rangle$ assumes a Pe-independent plateau. These considerations emphasize that the discrepancy between the eigenfunction and path integral solutions for $Pe \gtrsim 5$ (Fig. 4) is solely due to the neglect of higher order derivatives and not due to the neglect of the thermal contribution in Eq. (25).

The emergence and influence of torsion on the ABPO properties have not been investigated so far. However, our path integral formulation reveals an impact of twist on the ABPO conformations, specifically for semiflexible and stiff polymers. Moreover, simulation studies of polar active polymers—they are driven by active forces along the bonds[10,62]—yield a non-zero torsional angle, which increases with increasing activity.[63]

VII. CONCLUSIONS AND OUTLOOK

We have derived a path integral representation for the conformational properties of a semiflexible active Brownian polymer based on its stationary-state distribution function of the normal mode amplitudes. The normal mode amplitudes themselves are obtained as stationary-state solution of the Langevin equation of the ABPO.[31] The linearity of the ABPO equations of motion and the Gaussian nature of the stochastic process (Ornstein–Uhlenbeck process) yield a Gaussian distribution function of the normal mode amplitudes, which are transformed into a path integral for the continuous polymer. The latter includes characteristic semiflexible polymer contributions from entropy and bending energy, with activity dependent coefficients, and, in addition, activity-induced torsional and higher order correlations along the polymer contour. Neglecting torsional and higher order correlations, we obtain a path integral reminiscent of a semiflexible polymer with activity dependent coefficients. The comparison of the conformational properties obtained within the path integral representation with the result of the dynamical equations of motion yields good qualitative and even quantitative agreement over a considerable range of Péclet numbers. However, our calculations reveal the emergence of torsional contributions to the ABPO conformations, an aspect that needs to be analyzed in more detail.

Based on path integral representation, established procedures and approaches can be applied to analyze and characterize the out-of-equilibrium properties of active Brownian polymers. In particular, the differences to a strict semiflexible polymer are visible. Although not all conformational aspects of the ABPO are captured by the semiflexible polymer approximation, the path integral reveals that the ABPO conformational properties are determined by correlations of the active velocity, i.e., the colored noise process with the

correlations (6). This is in contrast to passive polymers, where the conformations are governed by white noise [Eq. (5)].

AUTHOR DECLARATIONS

Conflict of Interest

The authors have no conflicts to disclose.

DATA AVAILABILITY

The data that support the findings of this study are available from the corresponding author upon reasonable request.

APPENDIX: TRANSFORMATION OF SUM OVER MODES TO INTEGRAL OVER POSITIONS

We briefly illustrate the steps in the transformation of the sum-over-modes, Eq. (19), to the path integral representation of Eq. (24). Using the orthonormality

$$\int_{-L/2}^{L/2} \varphi_n(s)\varphi_m(s)ds = \delta_{nm} \tag{A1}$$

of the eigenfunctions, the left-hand side of Eq. (22) can be written as

$$\begin{aligned}\sum_n \xi_n \boldsymbol{\chi}_n^T \boldsymbol{\chi}_n &= \int_{-L/2}^{L/2} \sum_n \sum_m \xi_m \boldsymbol{\chi}_n^T \boldsymbol{\chi}_m \varphi_n(s)\varphi_m(s)ds \\ &= \int_{-L/2}^{L/2} \left(\sum_n \boldsymbol{\chi}_n^T \varphi_n(s)\right)\left(\sum_m \xi_m \boldsymbol{\chi}_m \varphi_m(s)\right)ds \\ &= \int_{-L/2}^{L/2} \boldsymbol{r}^T(s)\,\mathcal{O}\left(\sum_m \boldsymbol{\chi}_m \varphi_m(s)\right)ds \\ &= \int_{-L/2}^{L/2} \boldsymbol{r}^T(s)\,\mathcal{O}\,\boldsymbol{r}(s)ds. \end{aligned} \tag{A2}$$

Insertion of the differential operator (23) yields

$$\int_{-L/2}^{L/2} \boldsymbol{r}^T(s)(\mathcal{O}\,\boldsymbol{r}(s))ds = k_B T \int_{-L/2}^{L/2} \boldsymbol{r}^T(s)\left(\epsilon\frac{\partial^4}{\partial s^4} - 2\nu\frac{\partial^2}{\partial s^2}\right)\boldsymbol{r}(s)ds. \tag{A3}$$

Considering the term with the second derivative, partial integration yields

$$\int_{-L/2}^{L/2} \boldsymbol{r}\cdot\frac{\partial^2 \boldsymbol{r}}{\partial s^2}ds = \left(\boldsymbol{r}\cdot\frac{\partial \boldsymbol{r}}{\partial s}\right)_{-L/2}^{L/2} - \int_{-L/2}^{L/2}\left(\frac{\partial \boldsymbol{r}}{\partial s}\right)^2 ds.$$

Similarly, for the term with the fourth-order derivative, twice partial integration gives

$$\begin{aligned}\int_{-L/2}^{L/2} \boldsymbol{r}\cdot\frac{\partial^4 \boldsymbol{r}}{\partial s^4}ds &= \left(\boldsymbol{r}\cdot\frac{\partial^3 \boldsymbol{r}}{\partial s^3}\right)_{-L/2}^{L/2} - \left(\frac{\partial \boldsymbol{r}}{\partial s}\cdot\frac{\partial^2 \boldsymbol{r}}{\partial s^2}\right)_{-L/2}^{L/2} \\ &\quad + \int_{-L/2}^{L/2}\left(\frac{\partial^2 \boldsymbol{r}}{\partial s^2}\right)^2 ds.\end{aligned}$$

Using the boundary conditions [Eqs. (2) and (3)], Eq. (A3) becomes

$$\begin{aligned}&\int_{-L/2}^{L/2} \boldsymbol{r}^T\left(\epsilon\frac{\partial^4}{\partial s^4} - 2\nu\frac{\partial^2}{\partial s^2}\right)\boldsymbol{r}ds \\ &\quad = 2\nu\int_{-L/2}^{L/2}\left(\frac{\partial \boldsymbol{r}}{\partial s}\right)^2 ds + \epsilon\int_{-L/2}^{L/2}\left(\frac{\partial^2 \boldsymbol{r}}{\partial s^2}\right)^2 ds \\ &\quad\quad + 2\nu_0\left[\left(\frac{\partial \boldsymbol{r}}{\partial s}\right)_{L/2}^2 + \left(\frac{\partial \boldsymbol{r}}{\partial s}\right)_{-L/2}^2\right].\end{aligned} \tag{A4}$$

Analogously following Eq. (21) and inserting the operator $\mathcal{O}$ yield

$$\begin{aligned}\frac{1}{(k_B T)^2}\sum_n \xi_n^2 \boldsymbol{\chi}_n^T \boldsymbol{\chi}_n &= 4\nu^2\int_{-L/2}^{L/2}\left(\frac{\partial^2 \boldsymbol{r}}{\partial s^2}\right)^2 ds - 4\nu\epsilon\int_{-L/2}^{L/2}\frac{\partial^2 \boldsymbol{r}}{\partial s^2} \\ &\quad\cdot\frac{\partial^4 \boldsymbol{r}}{\partial s^4}ds + \epsilon^2\int_{-L/2}^{L/2}\left(\frac{\partial^4 \boldsymbol{r}}{\partial s^4}\right)^2 ds.\end{aligned}$$

Partial integration of the contribution with the product of the second and fourth derivative yields

$$\begin{aligned}\frac{1}{(k_B T)^2}\sum_n \xi_n^2 \boldsymbol{\chi}_n^T \boldsymbol{\chi}_n &= 4\nu^2\int_{-L/2}^{L/2}\left(\frac{\partial^2 \boldsymbol{r}}{\partial s^2}\right)^2 ds + 4\nu\epsilon\int_{-L/2}^{L/2}\left(\frac{\partial^3 \boldsymbol{r}}{\partial s^3}\right)^2 ds \\ &\quad + \epsilon^2\int_{-L/2}^{L/2}\left(\frac{\partial^4 \boldsymbol{r}}{\partial s^4}\right)^2 ds + \frac{16\nu_0\nu^2}{\epsilon} \\ &\quad\times\left[\left(\frac{\partial^2 \boldsymbol{r}}{\partial s^2}\right)_{-L/2}^2 + \left(\frac{\partial^2 \boldsymbol{r}}{\partial s^2}\right)_{L/2}^2\right].\end{aligned} \tag{A5}$$

The combination of Eqs. (19), (20), (A2), (A4), and (A5) yields Eq. (24).

REFERENCES

[1] Y. Demirel, J. Non-Newtonian Fluid Mech. **165**, 953 (2010).
[2] X. Fang, K. Kruse, T. Lu, and J. Wang, Rev. Mod. Phys. **91**, 045004 (2019).
[3] R. Kapral, J. Chem. Phys. **138**, 020901 (2013).
[4] R. Kapral and A. S. Mikhailov, Physica D **318–319**, 100 (2016).
[5] M. C. Marchetti, J. F. Joanny, S. Ramaswamy, T. B. Liverpool, J. Prost, M. Rao, and R. A. Simha, Rev. Mod. Phys. **85**, 1143 (2013).
[6] J. Elgeti, R. G. Winkler, and G. Gompper, Rep. Prog. Phys. **78**, 056601 (2015).
[7] F. Jülicher, S. W. Grill, and G. Salbreux, Rep. Prog. Phys. **81**, 076601 (2018).
[8] V. Hakim and P. Silberzan, Rep. Prog. Phys. **80**, 076601 (2017).
[9] A. Be'er and G. Ariel, Mov. Ecol. **7**, 9 (2019).
[10] R. G. Winkler and G. Gompper, J. Chem. Phys. **153**, 040901 (2020).
[11] C. P. Brangwynne, G. H. Koenderink, F. C. MacKintosh, and D. A. Weitz, J. Cell Biol. **183**, 583 (2008).
[12] C. A. Weber, R. Suzuki, V. Schaller, I. S. Aranson, A. R. Bausch, and E. Frey, Proc. Natl. Acad. Sci. U. S. A. **112**, 10703 (2015).
[13] A. W. C. Lau, B. D. Hoffman, A. Davies, J. C. Crocker, and T. C. Lubensky, Phys. Rev. Lett. **91**, 198101 (2003).
[14] F. C. MacKintosh and A. J. Levine, Phys. Rev. Lett. **100**, 018104 (2008).
[15] W. Lu, M. Winding, M. Lakonishok, J. Wildonger, and V. I. Gelfand, Proc. Natl. Acad. Sci. U. S. A. **113**, E4995 (2016).
[16] A. Ravichandran, G. A. Vliegenthart, G. Saggiorato, T. Auth, and G. Gompper, Biophys. J. **113**, 1121 (2017).
[17] D. Saintillan, M. J. Shelley, and A. Zidovska, Proc. Natl. Acad. Sci. U. S. A. **115**, 11442 (2018).
[18] M. Guthold, X. Zhu, C. Rivetti, G. Yang, N. H. Thomson, S. Kasas, H. G. Hansma, B. Smith, P. K. Hansma, and C. Bustamante, Biophys. J. **77**, 2284 (1999).

[19]Y. X. Mejia, E. Nudler, and C. Bustamante, Proc. Natl. Acad. Sci. U. S. A. **112**, 743 (2015).
[20]V. Belitsky and G. M. Schütz, Phys. Rev. E **99**, 012405 (2019).
[21]S. C. Weber, A. J. Spakowitz, and J. A. Theriot, Proc. Natl. Acad. Sci. U. S. A. **109**, 7338 (2012).
[22]A. Javer, Z. Long, E. Nugent, M. Grisi, K. Siriwatwetchakul, K. D. Dorfman, P. Cicuta, and M. Cosentino Lagomarsino, Nat. Commun. **4**, 3003 (2013).
[23]A. Zidovska, D. A. Weitz, and T. J. Mitchison, Proc. Natl. Acad. Sci. U. S. A. **110**, 15555 (2013).
[24]E. Lieberman-Aiden, N. L. van Berkum, L. Williams, M. Imakaev, T. Ragoczy, A. Telling, I. Amit, B. R. Lajoie, P. J. Sabo, M. O. Dorschner, R. Sandstrom, B. Bernstein, M. A. Bender, M. Groudine, A. Gnirke, J. Stamatoyannopoulos, L. A. Mirny, E. S. Lander, and J. Dekker, Science **326**, 289 (2009).
[25]T. Cremer, M. Cremer, B. Hübner, H. Strickfaden, D. Smeets, J. Popken, M. Sterr, Y. Markaki, K. Rippe, and C. Cremer, FEBS Lett. **589**, 2931 (2015).
[26]I. Solovei, K. Thanisch, and Y. Feodorova, Curr. Opin. Cell Biol. **40**, 47 (2016).
[27]M. Di Pierro, D. A. Potoyan, P. G. Wolynes, and J. N. Onuchic, Proc. Natl. Acad. Sci. U. S. A. **115**, 7753 (2018).
[28]A. Ghosh and N. S. Gov, Biophys. J. **107**, 1065 (2014).
[29]H. Vandebroek and C. Vanderzande, Phys. Rev. E **92**, 060601 (2015).
[30]N. Samanta and R. Chakrabarti, J. Phys. A: Math. Theor. **49**, 195601 (2016).
[31]T. Eisenstecken, G. Gompper, and R. G. Winkler, Polymers **8**, 304 (2016).
[32]T. Eisenstecken, G. Gompper, and R. G. Winkler, J. Chem. Phys. **146**, 154903 (2017).
[33]D. Osmanović and Y. Rabin, Soft Matter **13**, 963 (2017).
[34]S. Chaki and R. Chakrabarti, J. Chem. Phys. **150**, 094902 (2019).
[35]A. Martín-Gómez, G. Gompper, and R. G. Winkler, Polymers **10**, 837 (2018).
[36]S. M. Mousavi, G. Gompper, and R. G. Winkler, J. Chem. Phys. **150**, 064913 (2019).
[37]J. Harder, C. Valeriani, and A. Cacciuto, Phys. Rev. E **90**, 062312 (2014).
[38]D. Sarkar, S. Thakur, Y.-G. Tao, and R. Kapral, Soft Matter **10**, 9577 (2014).
[39]J. Shin, A. G. Cherstvy, W. K. Kim, and R. Metzler, New J. Phys. **17**, 113008 (2015).
[40]A. Martín-Gómez, T. Eisenstecken, G. Gompper, and R. G. Winkler, Soft Matter **15**, 3957 (2019).
[41]S. Das and A. Cacciuto, Phys. Rev. Lett. **123**, 087802 (2019).
[42]A. Martin-Gomez, T. Eisenstecken, G. Gompper, and R. G. Winkler, Phys. Rev. E **101**, 052612 (2020).
[43]S. K. Anand and S. P. Singh, Phys. Rev. E **101**, 030501 (2020).
[44]S. M. Mousavi, G. Gompper, and R. G. Winkler, J. Chem. Phys. **155**, 044902 (2021).
[45]E. F. Teixeira, H. C. M. Fernandes, and L. G. Brunnet, Soft Matter **17**, 5991 (2021).
[46]M. G. Bawendi and K. F. Freed, J. Chem. Phys. **83**, 2491 (1985).
[47]S. M. Battacharjee and M. Muthukumar, J. Chem. Phys. **86**, 411 (1987).
[48]J. B. Langowski, J. Noolandi, and B. Nickel, J. Chem. Phys. **95**, 1266 (1991).
[49]R. G. Winkler, P. Reineker, and L. Harnau, J. Chem. Phys. **101**, 8119 (1994).
[50]L. Harnau, R. G. Winkler, and P. Reineker, J. Chem. Phys. **102**, 7750 (1995).
[51]B. Y. Ha and D. Thirumalai, J. Chem. Phys. **103**, 9408 (1995).
[52]R. G. Winkler, J. Chem. Phys. **118**, 2919 (2003).
[53]R. G. Winkler and P. Reineker, Macromolecules **25**, 6891 (1992).
[54]R. G. Winkler, J. Chem. Phys. **133**, 164905 (2010).
[55]A. P. Solon, J. Stenhammar, R. Wittkowski, M. Kardar, Y. Kafri, M. E. Cates, and J. Tailleur, Phys. Rev. Lett. **114**, 198301 (2015).
[56]R. G. Winkler, Soft Matter **12**, 3737 (2016).
[57]S. Das, G. Gompper, and R. G. Winkler, New J. Phys. **20**, 015001 (2018).
[58]H. Risken, *The Fokker-Planck Equation* (Springer, Berlin, 1989).
[59]K. F. Freed, Adv. Chem. Phys. **22**, 1 (1972).
[60]H. Kleinert, *Path Integrals in Quantum Mechanics, Statistics, Polymer Physics, and Financial Markets* (World Scientific, Singapore, 1990).
[61]K. Kroy and E. Frey, Phys. Rev. E **55**, 3092 (1997).
[62]R. G. Winkler, J. Elgeti, and G. Gompper, J. Phys. Soc. Jpn. **86**, 101014 (2017).
[63]S. K. Anand and S. P. Singh, Phys. Rev. E **98**, 042501 (2018).